Preliminary Spallation Neutron Source Corrosion Experiments:

Corrosion Rates of Engineering Materials in a Water Degrader Cooling Loop Irradiated by an 800 MeV Proton Beam

R. Scott Lillard and Darryl P. Butt
Materials Corrosion & Environmental Effects Lab
MST-6, Metallurgy
Los Alamos National Laboratory
Los Alamos, New Mexico 87545

January, 1996

contributors:
Walter F. Sommer Jr., *MST-4*
Robert D. Brown, *AOT-7*
Robert E. Jones, *AOT-7*
Joseph L. Raybun, *AOT-7*

Executive Summary

PROJECT OBJECTIVES: The primary objective of this project was to demonstrate a capability to measure the corrosion rates of several engineering materials in a system that presented some of the obstacles we anticipate meeting in the summer of 1996 on a prototypical spallation neutron source. To accomplish this, it was necessary to: **1)** develop a corrosion probe / electrode system that could be used in a cooling water loop and with stand a radiation environment, **2)** develop a "floating"[1] - portable corrosion measurement system and, **3)** develop a data analysis model so that corrosion rates could be obtained from the measurement system. This report presents our progress in these areas.

EXPERIMENTAL: The corrosion probe developed for these experiments is shown in Figure 1. It is a 3/4-inch NPT pipe plug that acts as an electrical feed through for the samples to be monitored. In this probe, the corrosion samples are screwed down onto threaded studs which are electrically isolated from one another as well as from the surrounding pipe plug by a metal to glass seal. The

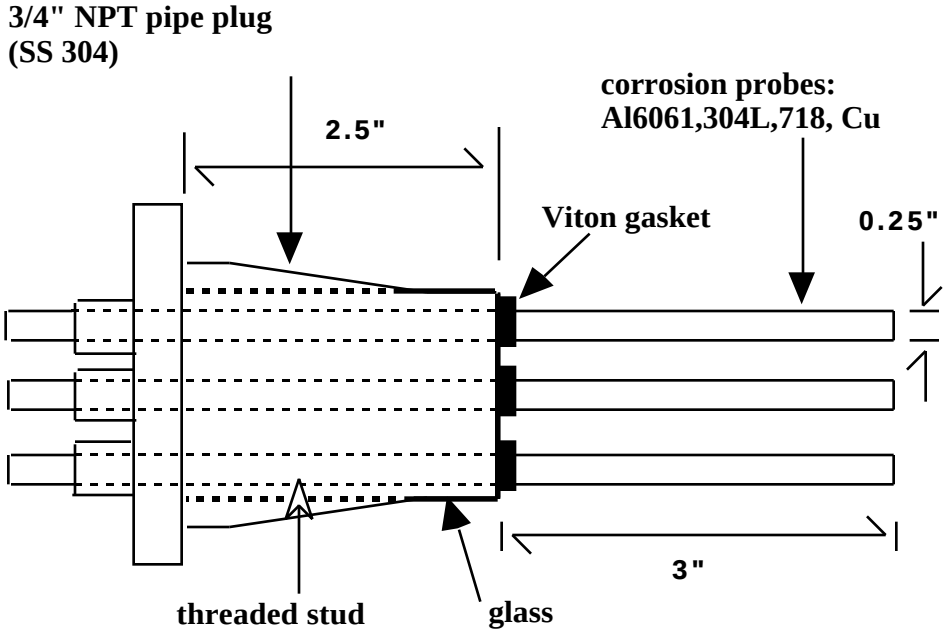

Figure 1 Schematic "representation" of the corrosion probe / electrode system

corrosion samples chosen for this study were: 304L Stainless Steel (SS 304L), Inconel 718 (Inc. 718), Aluminum 6061 (Al6061) and, copper (Cu).

The materials chosen for evaluation are all found in the degrader cooling water loop at the LANSCE A6 target station water degrader. This water degrader was continuously irradiated by an 800 MeV proton beam running at $1x10^{-3}$ Amps. The cooling loop had a nominal flow of 3-6 gallons per minute and a temperature of approximately 70° C. This loop was fitted with corrosion probes on both the inlet and outlet side of the degrader as shown in Figure 2 approximately 11 feet above the degrader / proton beam.

---

[1] The term floating is used here to denote the ground state of the instrument. Because the cooling water loop is earthed it is in contact with the electrical ground in traditional, non-floating, instruments.

The corrosion rates of the samples in the degrader cooling loop were measured as a function of immersion time with a technique know as Electrochemical Impedance Spectroscopy (EIS). EIS was chosen because it is a non-destructive method that allows the separation of the polarization resistance (which is directly proportional to corrosion rate) from the solution resistance which act together in series. It is important to be able to quantify the solution resistance in the degrader cooling loop for two reasons 1) the solution resistivity may be obtained from this measurement and 2) because its value will be large if it must be subtracted from the data. Because the polarization resistance and solution resistance act together in series traditional dc techniques measure the sum of these two resistances. If the solution resistance is large relative to the polarization resistance (which is the case for the de-ionized water in the cooling loop) an under estimation of the corrosion rate will result. However, ac techniques (such as EIS) take advantage of the double layer capacitance formed at a metal interface in solution. This capacitance acts in parallel to the polarization resistance. At high perturbation frequencies all of the current flows through the capacitor and the solution resistance is measured. At low frequencies (near dc) all of the current flows through the polarization resistance and the sum of the polarization resistance and the solution resistance are measured.

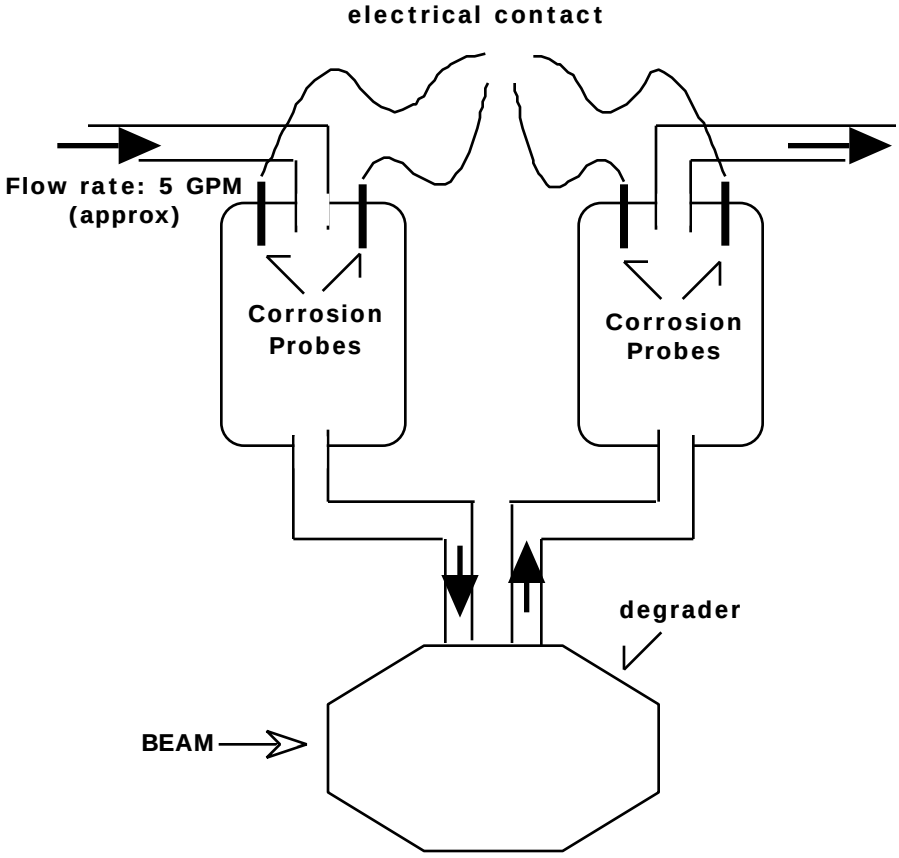

Figure 2 Schematic "representation" of the degrader cooling water loop at the A6 target station of LANSCE showing the placement of the corrosion probes.

The portable EIS system used in this study consisted of Frequency Response Analyzer and Potentiostat boards which fit into the expansion slots of a "luggable" computer. This system gave the versatility needed to make measurements in a working environment (i.e. outside of the lab). It was also capable of making electrically isolated

measurements which is important in the "real world" to eliminate artifacts caused by the currents/voltages found in all grounded systems such as water pipes.

RESULTS AND DISCUSSIONS: The corrosion rates of stainless steel 304L, Inconel 718, aluminum 6061, and copper were monitored as a function of immersion time in the degrader cooling water loop between August and November of 1995. The results of the return stream measurements are summarized in Figure 3. In calculating these rates it was assumed that corrosion was occurring uniformly over the sample surface. The letters **E** and **O** on this plot represent a common assignment for corrosion resistance based on failure rates of ferrous and nickel based alloys (Table 1). Assuming uniform corrosion, all of these materials exhibit Outstanding to Excellent corrosion resistance. However, these rates are likely non-

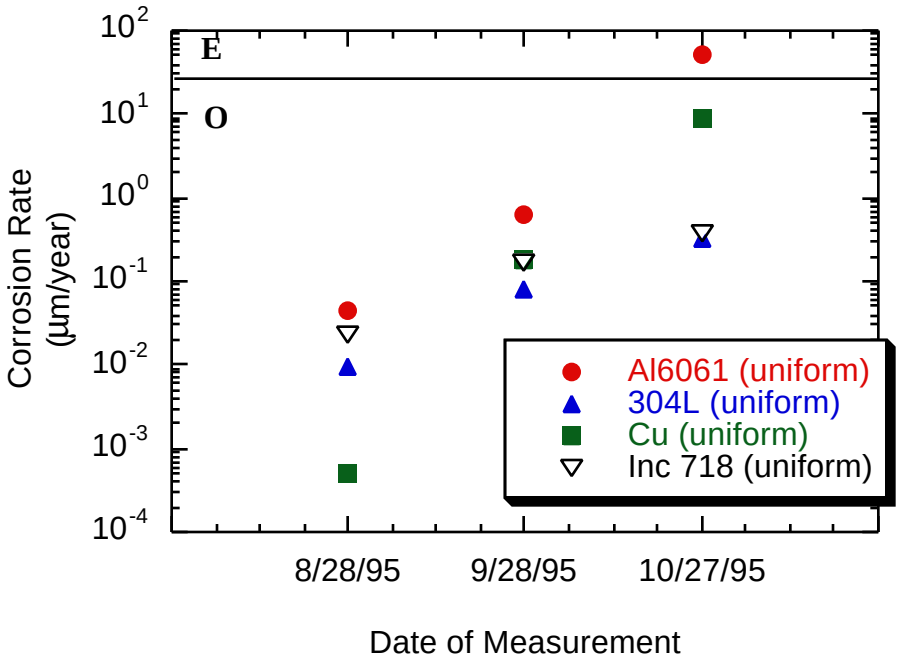

Figure 3 Corrosion rates for samples on the return side of the degrader as a function of immersion time. All rates in this plot assume uniform corrosion over the sample surface.

Table 1 Designations for corrosion resistance based on failure rates of ferrous and nickel based alloys

Relative Corrosion Resistance	Metric Units µm/year	English Units mils/year	Current Density for Steel in mA/cm^2
Outstanding	<25	<1	<2.2x10^{-3}
Excellent	25-100	1-5	2.2 - 11 x10^{-3}
Good	100-500	5-20	11 - 44 x10^{-3}
Fair	500-1000	20-50	4.4 - 11.0 x10^{-2}
Poor	1000-5000	50-200	11.0 - 44.0 x10^{-2}

UnAcceptable	>5000	>200	>44.0 x10^{-2}

conservative as rarely is corrosion a uniform process. To account for this, the rates were also calculated assuming most of the corrosion current originated from several small pits (1mm^2) on the surface of the sample (Figure 4). With this more conservative assumption, Inc. 718 and SS 304L still exhibit outstanding corrosion resistance over the test period of 4 months. However, Al6061, was found to corrode at an appreciable rate by the end of the test period, approximately 2,600 µm/yr. This rate is high and will require additional scrutiny in future experiments especially if this is a candidate material for helium transfer tubes in APT. Post Mortem inspection of the corrosion samples will give us a better indication of the actual pit density.

A comparison between the corrosion rates of Cu in the supply and return streams is presented in Figure 5. As clearly seen in this figure, the corrosion rate in the return stream is almost 5 times greater than that in the supply stream. It is believed that this difference owes to the formation of hydrogen peroxide a known water radiolysis product. Hydrogen peroxide is formed from the combination of 2 OH radicals:

$$OH + OH \xrightarrow{k_{H_2O_2}} H_2O_2 \quad k_{H_2O_2} = 4x10^9$$

It is hoped that peroxide formation and can be mitigated by using "Hydrogen Water Chemistry" currently used in operating boiling water reactors. By bubbling H_2 gas into the cooling water the OH radical is preferentially transformed into water:

$$OH + H \xrightarrow{k_{H_2O}} H_2O \quad k_{H_2O} = 2.4x10^{10}$$

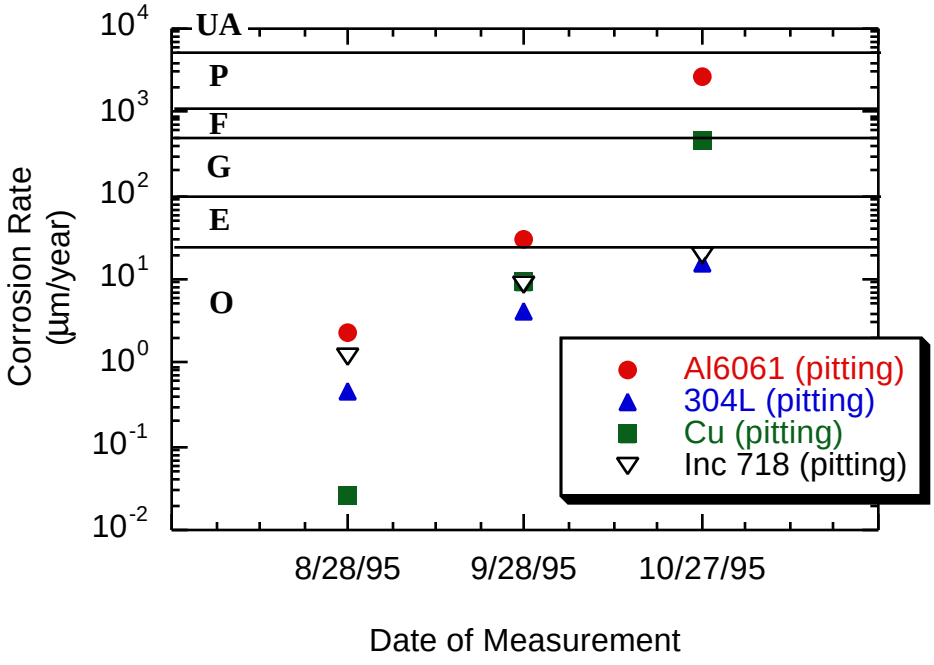

Figure 4 Corrosion rates for samples on the return side of the degrader as a function of immersion time. All rates in this plot assume localized corrosion on the sample surface.

As mentioned earlier, EIS allows one to measure solution resistance as a function of time. By calibrating a specially designed corrosion probe prior to placement in the cooling water loop, the solution resistivity was obtained from the EIS solution resistance data (Figure 6). The initial system water in this cooling loop was deionized and had a conductivity of approximately 10^{-6} (ohm cm)$^{-1}$. Approximately 2 weeks after irradiation of the degrader commenced (8/28/95) the measured conductivity was approximately 3 x10^{-4} (ohm cm)$^{-1}$. By the end of the test period the solution conductivity had increased even further to approximately 6 x10^{-4} (ohm cm)$^{-1}$. For comparison the resistivity of 1 millimolar

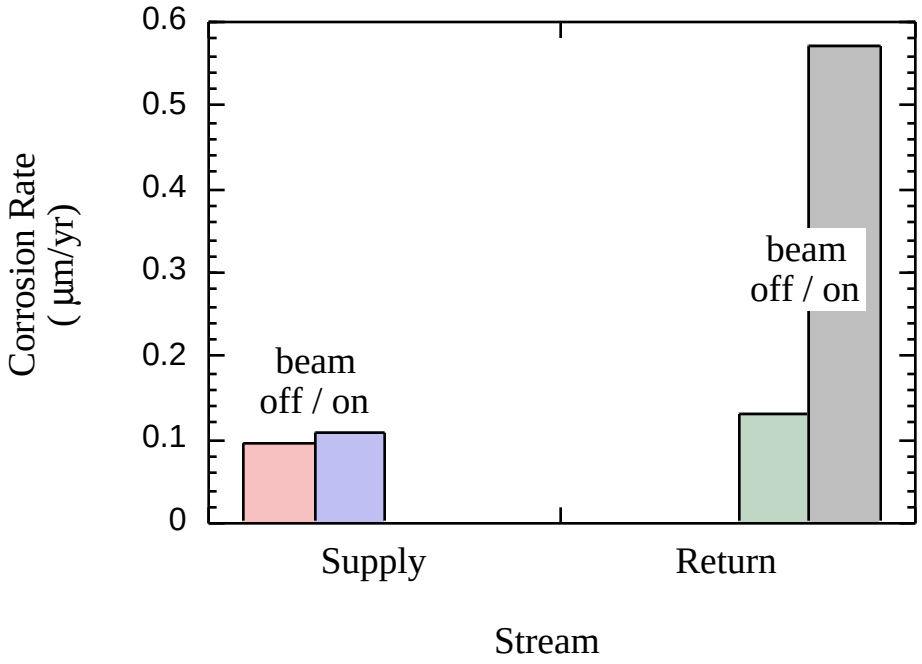

Figure 5 Comparison between supply and return stream corrosion rates for Cu electrodes. Plot shows both the beam off data (8/21/95) and beam on data (8/22/95) for the same electrodes.

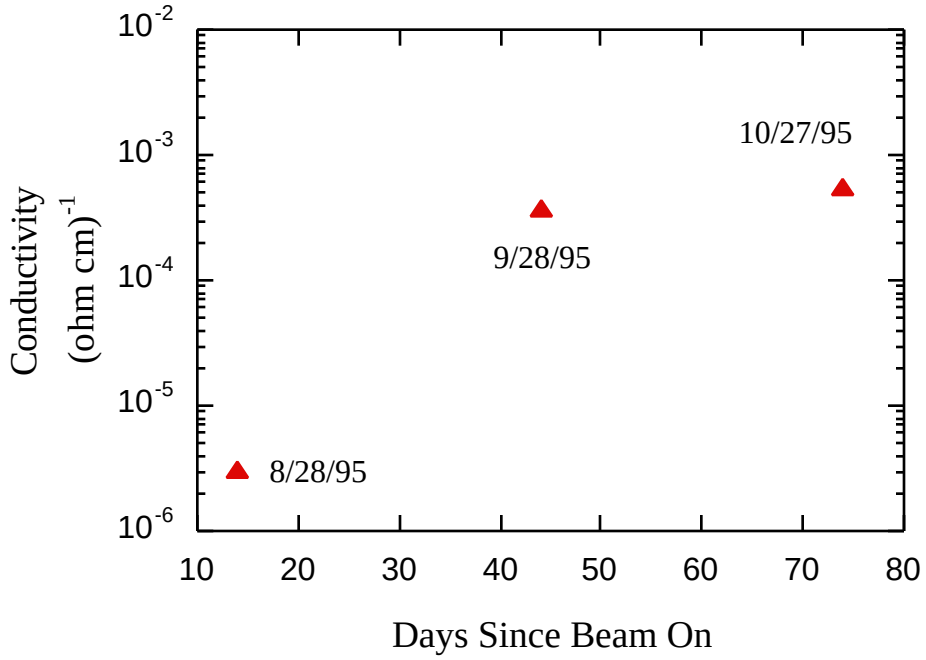

Figure 6 Measured solution conductivity as a function of beam time.

NaCl is approximately 1.2 x10^{-3} (ohm cm)$^{-1}$. The observation that both the corrosion resistance of the samples decrease with time and the solution conductivity measurements increase with time is not coincidental. The cooling water conductivity will increase with increasing concentrations of salts, metal ions (corrosion product) water radiolysis or a combination of the three.

SUMMARY OF ACCOMPLISHMENTS: This work has enabled us to prove our concept for a spallation target neutron source corrosion rate measurements to begin in the Summer of 1996. We have: **1)** developed a corrosion probe / electrodes that will operate reliably in a radioactive cooling water loop, **2)** developed a "floating" - portable corrosion measurement system that employs EIS a non-destructive technique for measuring corrosion rates and, **3)** developed a data analysis model so that corrosion rate and solution resistivity can be measured in the APT prototypical environment. The corrosion measurement system was demonstrated by measuring the corrosion rates of various engineering materials in the cooling water loop for a water degrader in the A6 target station of LANSCE.

Results from this investigation show that Aluminum 6061 has a relatively high corrosion rate after 4 months of immersion in the degrader cooling water. Assuming that the corrosion is non-uniform (pitting) this alloy may be classified as **Poor**. In comparison, 304L SS and Inc. 718 maintain **Outstanding** to **Excellent** classifications during the test period even assuming a non-uniform (pitting) corrosion on the sample surface. The cooling water resistivity decreased by several orders of magnitude during the test period. This result corresponds to the corrosion rate measurements as it indicates a increase in dissolved salts and / radioactive species. It is well known that corrosion rate decreases with increasing concentrations of salts or radioactive species.

FUTURE WORK

- "Post Mortem" Analysis of Corrosion Electrodes to Determine Whether or not Pitting Corrosion Exists
- Development of "In Beam" Corrosion Probes to Allow Measurement of Corrosion Rates During Proton Irradiation
- Corrosion Rate Measurements of Proposed APT Materials (W, HT-9, 316NG, Inc. 718, Al6061) in a Prototypical Spallation Target Cooling Water Loop
- Examine the Effect of Hydrogen Water Chemistry on Corrosion Mitigation in a Prototypical Spallation Target Cooling Water Loop
- Development of a pH Probe to Measure Changes in Cooling Water pH during the Irradiation Period
- Exploration of Existing Boiling Water Reactor Reference Electrode Technology for use in Prototypical Spallation Target Cooling Water Loop
- Laboratory Corrosion Rate Measurements of Proposed APT Materials in Simulated Spallation Target Cooling Water
- Measure the Corrosion Rates of Potential Galvanic Couples in Simulated Spallation Target Cooling Water

List of Tables

List of Figures

Page Number

Table of Contents

Abstract

This report introduces a unique corrosion rate system that has been developed for APT. It consists of: **1)** corrosion probe / electrodes that will operate reliably in a radioactive cooling water loop, **2)** a "floating" - portable corrosion measurement system that employs a non-destructive technique for measuring corrosion rates, and **3)** a data analysis model so that corrosion rate and solution resistivity can be measured in the APT prototypical environment. This system was tested by measuring the corrosion rates of Al6061, Cu, Inconel 718, and 304L Stainless Steel in the cooling water loop for a degrader in the A6 pit area of LANSCE. Corrosion rate measurements on Cu electrodes in supply stream and return stream buckets placed on the have found that with the beam on, return stream corrosion rates were 5 times higher than supply stream rates. With the beam off, no difference between the supply and return stream corrosion rates was observed. In addition, the long term effects of water irradiation were found to increase cooling water conductivity by several orders of magnitude over the test period. Results from the cooling water loop corrosion rate measurements have also shown that aluminum 6061 has a relatively high corrosion rate after 4 months of immersion in the degrader cooling water. The corrosion resistance of this alloy was classified as **Fair** to **Unacceptable** depending on the data analysis method (localized corrosion vs. uniform corrosion). In comparison, stainless steel 304L and Inconel 718 maintain **Outstanding** to **Excellent** classifications during the test period even assuming a conservative non-uniform (pitting corrosion) analysis of the corrosion rates.

Introduction

The anticipated needs for tritium have called for an analysis of proton accelerator technologies as an alternative to reactor production. To produce tritium with an accelerator, a spallation target (typically tungsten or lead) is bombarded with high energy protons. As a result of this bombardment, neutrons are produced. The energy of these neutrons is moderated by interaction with water. Tritium is produced by capturing the moderated neutrons in helium (He-3 gas). To minimize its temperature and to provide a neutron moderator, the spallation target is immersed in a cooling water loop. Although the water to be used in the spallation target cooling loop will initially be distilled and deionized to reduce the concentration of aggressive anions, a build up of radiolysis products produced by the interaction of the proton beam with the cooling water will (neutron radiolysis) occur over time unless prevented.

Radiolysis model **[1**,**2**,**3]** have found that both oxidizing and reducing species are produced water is irradiated with proton, neutron, or gamma radiation. While many radicals are produced in this process, the species having the highest concentration after a few milliseconds is hydrogen peroxide (H_2O_2)**[4]**. Hydrogen peroxide, an oxidizing agent, is formed from the combination of 2 OH radicals produced during irradiation:

$$OH + OH \xrightarrow{k_{H_2O_2}} H_2O_2 \quad k_{H_2O_2} = 4x10^9$$

In cases where the rate of the corrosion reaction is cathodically limited the formation of peroxide can be particularly detrimental as its presence and its decomposition products (namely O_2), will increase the rate of the cathodic reaction. This results in a positive shift in the open circuit potential**[5]** and an increase in the corrosion rate**[6**,**7]**.It is believed that hydrogen peroxide formation can be mitigated in the neutron spallation target cooling loop

by using "Hydrogen Water Chemistry"**[8**,**9**,**10**,**11]** currently used in operating commercial boiling water reactors. By bubbling H_2 gas into the cooling water the OH radical preferentially reacts with dissolve (atomic) hydrogen to form water:

$$OH + H \xrightarrow{k_{H_2O}} H_2O \quad k_{H_2O} = 2.4x10^{10}$$

While some valuable insight of the effects of radiolysis products on corrosion rates has been gained through laboratory simulation**[12]**, many of the radiolysis products are short lived and difficult to reproduce in a laboratory environment. Therefore, a method for measuring the corrosion rates of candidate materials in a prototypical cooling water loop is preferable. To successfully measure the corrosion rate of the proposed materials in a prototypical APT cooling water loop the measurement system must have the following qualifications: 1) because the solution resistance will be very high the method must allow for it to be subtracted from the polarization resistance 2) to monitor only the effects of the cooling water loop on corrosion rate the method should be non-destructive 3) because the plumbing would act as an electrical sink for a traditionally grounded instrument the system must be isolated from ground (referred to as a "floating ground"), and 4) the system should be portable to allow it to be easily moved from location to location.

In traditional dc electrochemical techniques for measuring corrosion rate the solution resistance (R_{sol}) can be neglected if it is small relative to the polarization resistance (R_{pol} which is inversely proportional to corrosion rate); i.e. $V_{applied}/I_{meas} = R_{sol}+R_{pol}$. Typical values for R_{sol} are on the order 100 ohms or less where as R_{pol} is generally on the order of 10^6 ohms. The water used to cool the proton degrader is distilled and de-ionized prior to being pumped into the system. It has an initial conductivity of approximately 10^{-6} (ohm cm)$^{-1}$. The resultant solution resistance between two parallel plate electrodes 1 cm^2 in area

separated by 1 cm^2 would be 10^6 ohms. If this solution resistance is not corrected for, the polarization resistance for the materials in this solution will be over estimated, therefore, the corrosion rate will be underestimated.

Electrochemical Impedance Spectroscopy (EIS) is a powerful non-destructive technique for measuring the corrosion rates of metals in aqueous environments**[13**,**14**,**15]** and is ideally suited for systems with high solution resistivity. In EIS a small sinusoidal voltage perturbation (10 mV) is applied across the interface as a function of frequency. By measuring the transfer function of this applied ac voltage perturbation to the ac current response of the material, an impedance results ($Z\omega=V\omega/I\omega$). In the simplest sense, at low frequencies the material behaves as a resistor and $Z\omega=(R_{sol}+R_{pol})$. At high frequencies, the material behaves as a capacitor and, therefore, offers no resistance to current, and as a result $Z\omega=R_{sol}$. It is this high frequency behavior that allows the solution resistance to be subtracted from the polarization resistance. Because the ac voltage perturbation used in EIS is small (10 mV or less), it is a nondestructive technique and corrosion rates can be measured at the materials "free corrosion potential" (i.e. its open circuit potential). Traditional dc techniques rely on applied voltages of 100 mV or greater. These relatively high voltages damage the surface and accelerate the corrosion process.

This report demonstrates our capability to measure the corrosion rates of several engineering materials with EIS in a system that presents some of the obstacles we anticipate meeting on our prototypical APT system. It describes the corrosion probe / electrode system used and the EIS analysis models used to determine corrosion rates. Corrosion rates in radiated APT prototypical water as a function of time of exposure and position in the cooling water loop are also presented.

Experimental

Corrosion experiments were conducted on electrodes made from rod-shaped specimens of 304L stainless steel (304L SS) 18-20 at% Cr, 8-12 Ni, 2 Mn, bal. Fe; Inconel 718 (Inc. 718), 19% Cr, 18.5% Fe, 5% Nb, 3% Mo, bal. Ni; aluminum 6061 (Al6061), 1% Mg, 0.6 Si, 0.3 Mn; and 99.5% copper (Cu). Prior to exposure all specimens were polished to 800 grit SiC paper and then degreased with ethanol and cleaned with deionized water in an ultrasonic cleaner. These electrodes were mounted on a 3/4" NPT pipe plug which acted as a feed-through from the atmosphere to the pressurized cooling water loop. The 304L SS pipe plug was fitted with three threaded studs that were insulated from one another by a glass to metal seal (Figure 1). The rod-shaped electrodes (ranging from 2 to 5 cm^2) were tapped to accept the stud which also provided electrical contact. A Viton gasket between the electrode and the pipe plug prevented cooling water from contacting the stud. Two electrodes and one counter / pseudo-reference electrode made from Hastelloy C-276 (a Ni, Cr, Mo alloy which is very resistant to corrosion) were fitted to each feedthrough.

Corrosion probes were placed in "buckets" in the cooling

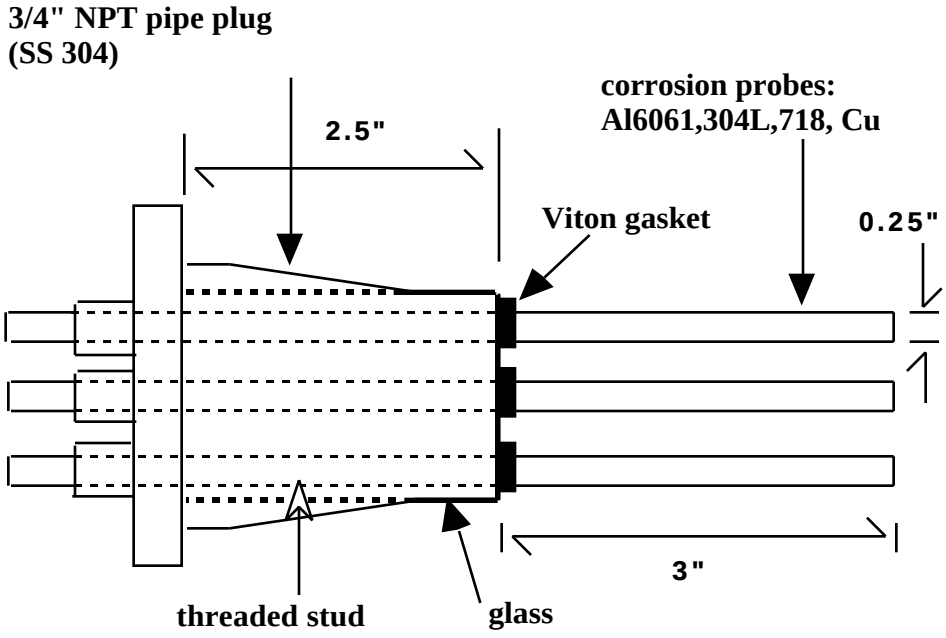

Figure 1 A schematic diagram of the corrosion probes and electrodes.

loop on both the supply side and return side of the proton beam degrader at the A6 area at LANSCE (Figure 2). The proton beam has an energy of approximately 800 MeV and a current of 1mA. The nominal water flow in the cooling loop is 5 gallons per minute. The degrader (being used for neutrino experiments) causes the water to have a resident time of approximately 16 seconds in the beam. Each bucket also contained a conductivity probe. This probe was constructed by placing C-276 electrodes of equal size on all three studs. These probes were calibrated as a function of solution volume and resistivity as discussed later in this report.

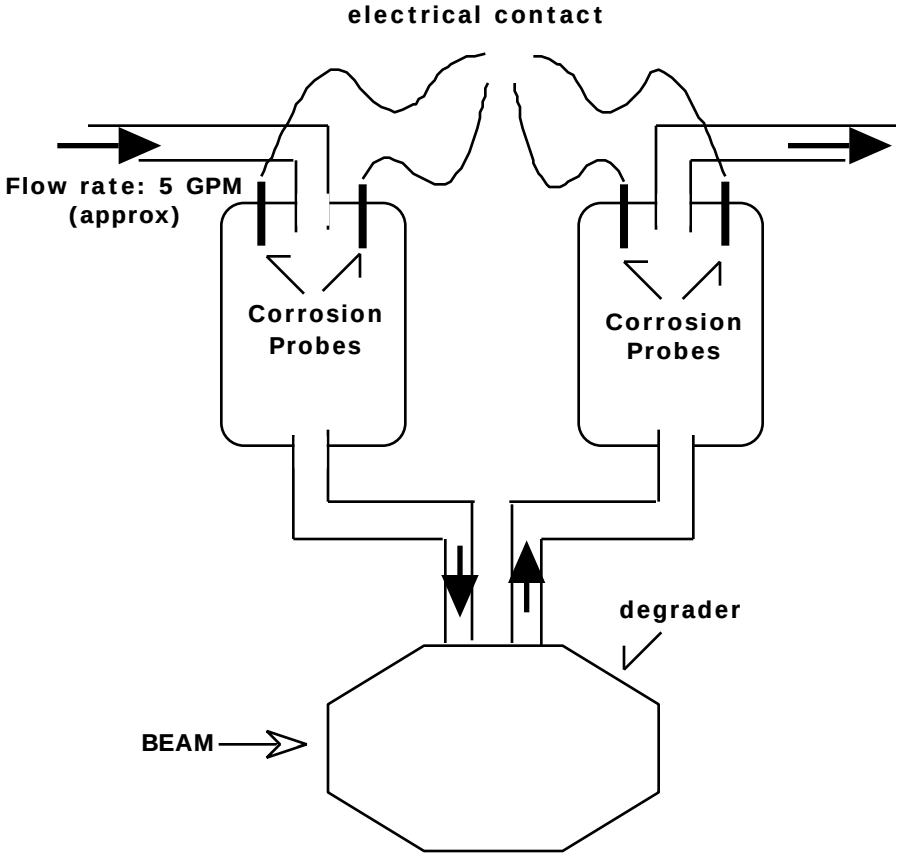

Figure 2 A schematic diagram showing the placement of corrosion probes in the A6 area at LANSCE

Corrosion rates were obtained from two electrode Electrochemical Impedance Spectroscopy (EIS) measurements, the C-276 acting as both the reference and counter

electrodes. Because both the cooling water loop and the working electrode in traditional laboratory instruments are grounded, a floating EIS system (Gamry Instruments EIS900) was used to eliminate ground loops. All EIS measurements were made at the Open Circuit Potential (OCP).

Results and Discussions

Calibration of EIS System To avoid exposure to lethal dosages of radiation, it was necessary to separate the corrosion test system (which was human operated) by a moderate distance and shielding. This called for cable lengths of about 120'. To insure that the capacitive and resistive characteristics of these relatively long cables were not affecting the corrosion measurements, the system was tested with a known resistance. Two coaxial cables identical length to those used with the corrosion probes were placed near one of the corrosion buckets, the center of each cable was connected by a 1K ohm resistor (Figure 3). The shields were grounded in the same manner as those in the corrosion measurements. Bode magnitude and phase plots for this 1K ohm resistor are presented in Figure 4. Although some phase shift was observed in the Bode phase plot above 10^4 Hertz (Hz), in the frequency range of 10^{-3} to 10^4 Hz the phase shift is approximately 0.0. Further, a resistance of 1K ohm is observed over the entire frequency range in the Bode magnitude plot. The response observed is that which was anticipated as the impedance of a resistor is equal to its dc resistance independent of perturbation frequency. From this data, it was concluded that the EIS measurements were not affected by cable length over the frequency range of 10^{-3} to 10^4 Hz. For this reason, all EIS measurements and data analysis were limited to this frequency range.

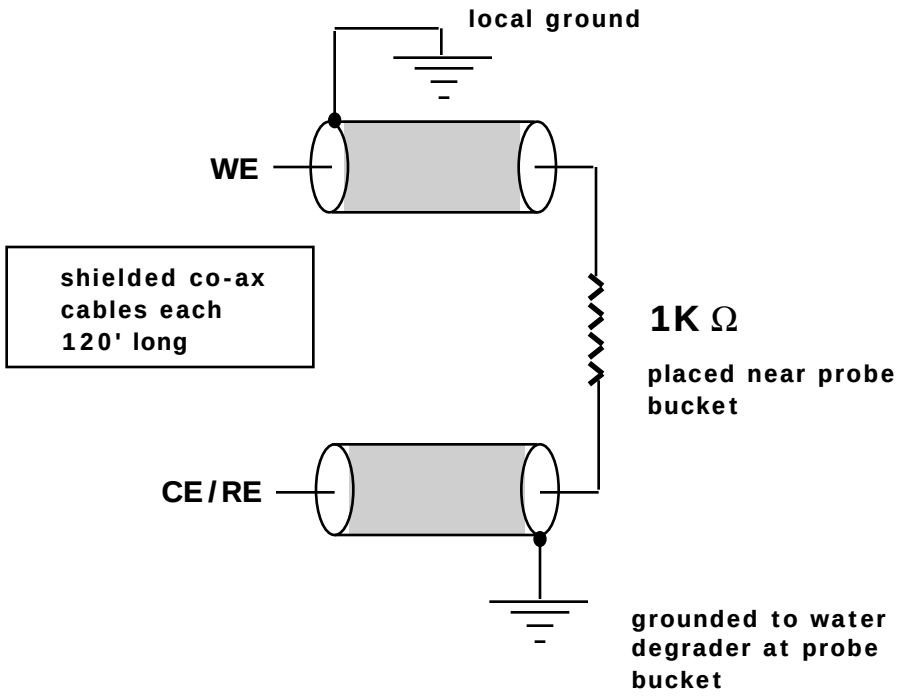

Figure 3 Schematic diagram of the cable system used to calibrate the EIS system.

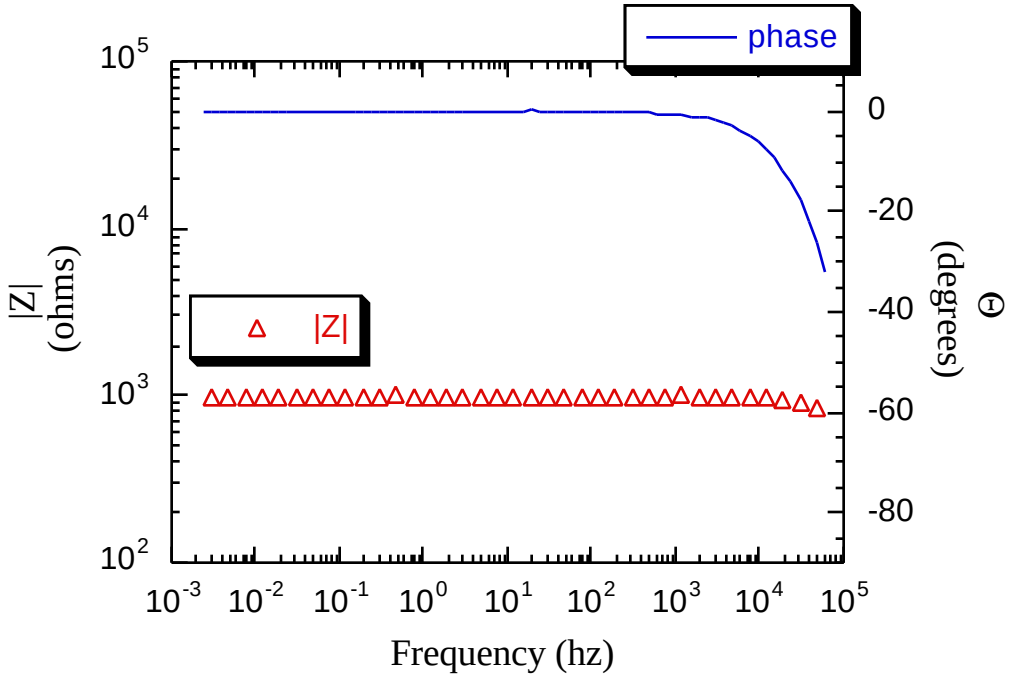

Figure 4 Bode Magnitude and phase plots for the cable calibration system depicted in Figure 3 above.

Corrosion Rates of Cooling Water Loop Materials (Return Stream) Typical Bode magnitude and phase plots for Al 6061 after approximately two weeks of beam time are presented in Figure 5. The same plots for 304L SS after six weeks of beam time are shown in Figure 6. The data shown were taken for probes on the return side of the beam. All of the EIS measurements exhibited two time constants. The low frequency time constant had a slope equal to -1/2 in the Bode Magnitude plot while the intermediate frequency time constant had a slope equal to -1. The equivalent circuit (EC) shown Figure 7 is one model which fits this type of response where R_{pol} represents the polarization resistance, C_{dl} is the double layer capacitance, R_{sol} is the solution resistance, and W represents the diffusion of reacting species to the surface. The polarization resistance can

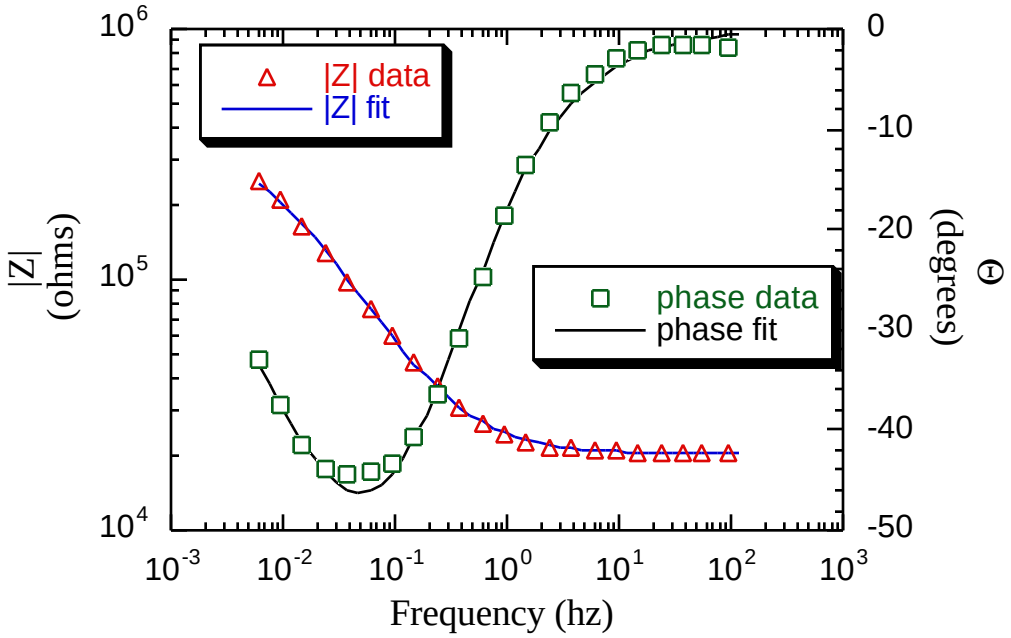

Figure 5 Bode magnitude and phase plots for Al 6061 on the return side of the proton degrader after 2 weeks of beam time (measurement date: 8/28/95)

be related to corrosion rate (CR) from the expression:

$$CR(\mu m / yr) = \frac{3.27x10^{6} \cdot \left(0.026 / R_{pol}\right)(E.W.)}{Den.} \qquad \text{Eq. 1}$$

where: E.W. is the equivalent weight and Den. is the density in grams/cm^3. The Warburg impedance (Z_w; W in Figure 7) is characterized by the relationship:

$$Z_w = \sigma\omega^{-1/2} - j\sigma\omega^{-1/2} \qquad \text{Eq. 2}$$

where σ is proportional to $1/D^{1/2}$ and D is a diffusion coefficient**[16]**. For this reason the Warburg impedance is referred to as a diffusional impedance. Equation 2 shows that Z_w is a function of $\omega^{-1/2}$, hence the slope of the Bode magnitude plots at low frequencies is -1/2 (Figures 3 and 4). The impedance of the double layer capacitance is related to frequency by

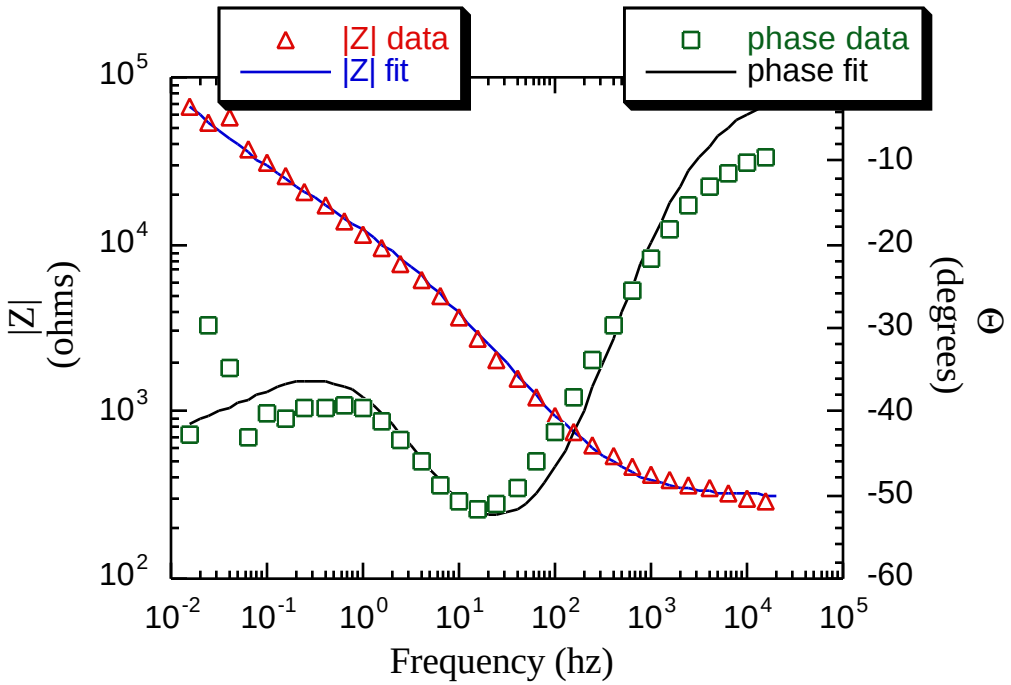

Figure 6 Bode magnitude and phase plots for 304L SS on the return side of the proton degrader after 2 months of beam time (measurement date: 10/27/95)

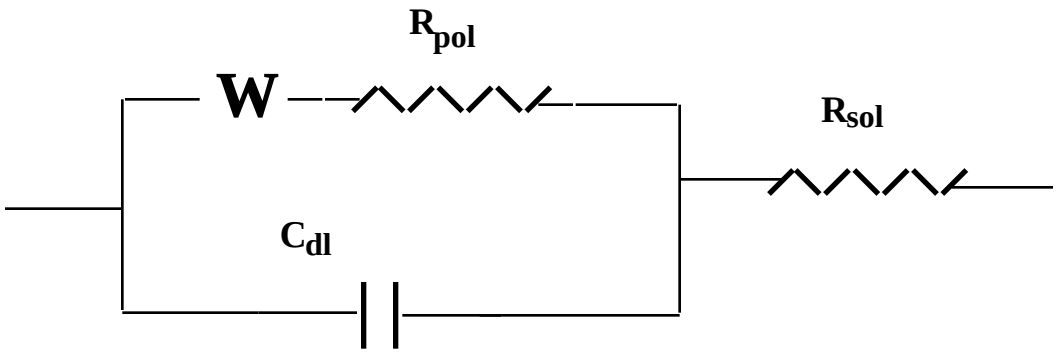

Figure 7 The equivalent circuit model used to model the EIS data.

the relationship:

$$Z_C = (j\omega C)^{-1} \qquad \text{Eq. 3}$$

where C is capacitance and $j=(-1)^{1/2}$. Equation 3 shows that the Z_C is a function of ω^{-1}, hence the slope of the Bode magnitude plot at intermediate frequencies is -1 (Figures 5 and 6).

The Bode data from all EIS measurements were modeled with the EC depicted in Figure 7. However, in order to more accurately determine the polarization resistance from the data, however, a constant phase element (R_{CPE}, α) was used in place of a double layer capacitance. Similar to C_{dl}, the CPE is proportional to $\omega^{-\Xi}$, where α is generally between 1 and 0.75 (for α =1, $Z_{cpe}=Z_c$). Typical results are shown in Figures 5 and 6 as solid lines. In general, good agreement between the data and the model existed, although, a few fits showed some deviation. The parameters from the fits presented in Figures 5 and 6 are shown in Table 1.

Because EIS is a surface averaged measurement, the true area over which corrosion is occurring is unknown. Therefore, if corrosion is localized (i.e. pitting corrosion), the

Table 1 Values of EC parameters (Figure 7) for Al 6061 and SS 304L corrosion probes after beam times of 2 weeks and 2 months respectively.

fit parameter	**value**	
	Al 6061	**SS 304L**
$\mathbf{R_{pol}}$	3.13×10^{5} ohms	1.29×10^{4} ohms
$\mathbf{R_{sol}}$	2.01×10^{4} ohms	310 ohms
$\mathbf{R_{cpe}}$	3.38×10^{4} ohms	9.41×10^{4} ohms
α	0.77	0.75
$\mathbf{R_W}$	9.45×10^{3} ohms	1.45×10^{4} ohms

corrosion rate obtained from EIS will under estimate the true rate (non-conservative). To account for this potential problem corrosion rates were determined using Equation 2 above and the fitted EIS polarization resistance data for two scenarios. Figure 8 presents CR as a function of beam time in the return stream assuming that corrosion is occurring uniformly over the entire sample surface. Therefore, this plot presents a "best case" scenario; e.g. the minimum corrosion rate of the sample in the return stream cooling water. For comparison,

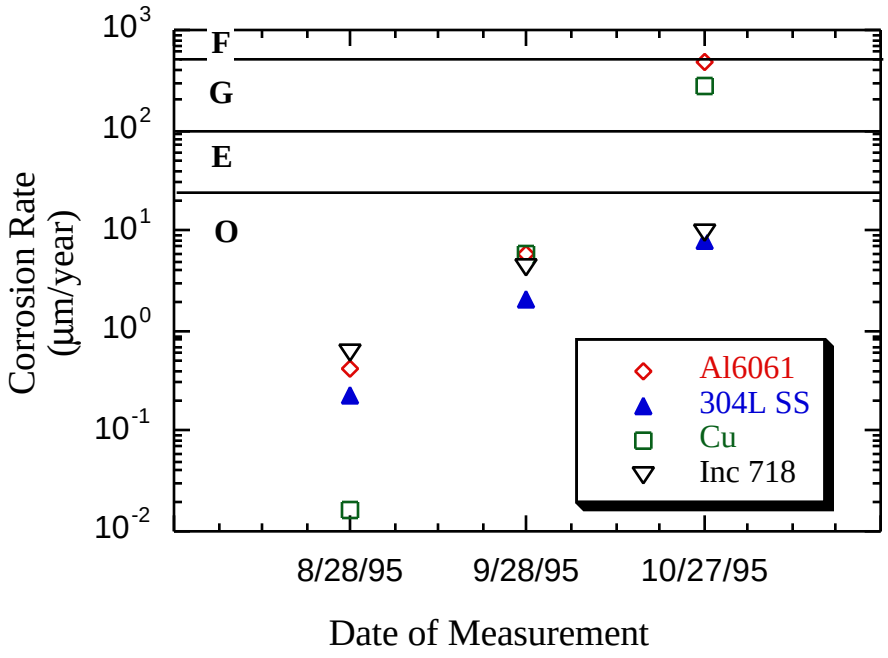

Figure 8 Corrosion rates of test samples as a function of beam time. Analysis assumes uniform corrosion over the sample surface.

relative boundaries separating areas of increasing corrosion resistance are shown on this plot. These boundaries are based on steel corrosion rates as shown in Table 2**[17]**. From this data, the following ranking of increasing corrosion resistance is obtained: Al6061 < Cu < Inconel 718 < SS 304L. Further, we might conclude that the corrosion resistance of Inconel 718 and SS 304L was "Outstanding" during the test period while that of Al6061

and Cu was “Good” to “Fair”. However, because corrosion is assumed to be uniform in this analysis, these rates are non-conservative.

A more conservative analysis of the corrosion rates of these materials is presented in Figure 9. This CR data was generated assuming that corrosion was only occurring over 2% of the sample’s surface area. A 2% active area is equivalent to 6-12 pits on the surface of the sample (actual number depends on the surface area of the sample). Each pit having an area equal to 1 mm^2. A post mortem analysis of the samples (to be completed at a later

Table 2 Designations for corrosion resistance based on failure rates of ferrous and nickel based alloys (From **[12]**)

Relative Corrosion Resistance	Metric Units μm/year	English Units mils/year	Current Density for Steel in mA/cm^2
UnAcceptable	>5000	>200	$>44.0 \times 10^{-2}$
Poor	1000-5000	50-200	$11.0 - 44.0 \times 10^{-2}$
Fair	500-1000	20-50	$4.4 - 11.0 \times 10^{-2}$
Good	100-500	5-20	$11 - 44 \times 10^{-3}$
Excellent	25-100	1-5	$2.2 - 11 \times 10^{-3}$
Outstanding	<25	<1	$<2.2 \times 10^{-3}$

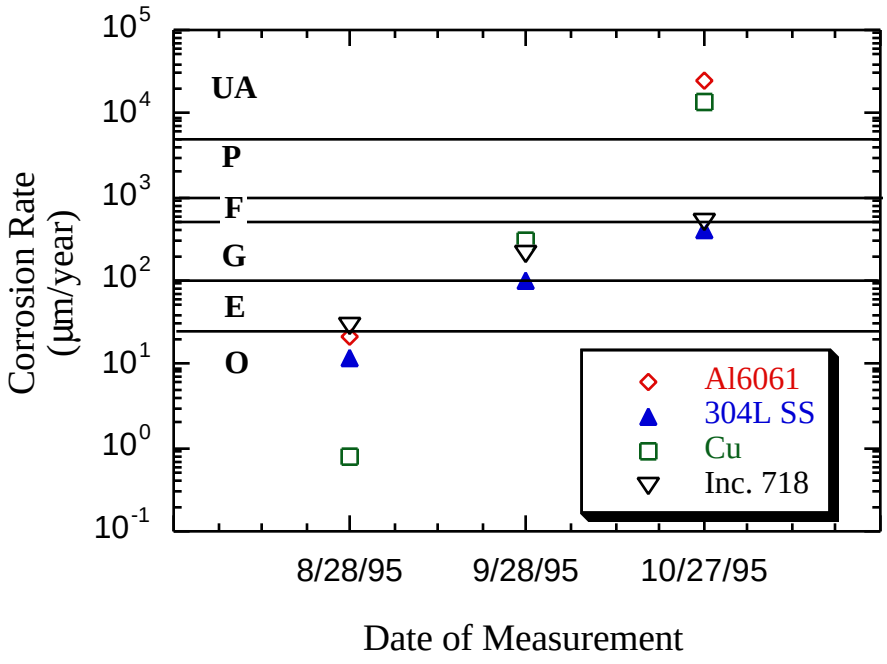

Figure 9 Corrosion rates of test samples as a function of beam time. Analysis assumes localized corrosion on the sample surface.

date) will reveal the validity of this assumption. Therefore, this analysis is more conservative and should be weighted proportionally. While the ranking of the relative corrosion resistances has not changed with this analysis, the apparent corrosion rates are approximately 50 times higher. In this analysis, the corrosion resistance of 304L SS and Inconel 718 was graded as Good to Fair while that of Cu and Al6061 was Unacceptable. These rates, however, should not be considered as absolute. More likely, they are an upper boundary for the actually corrosion rates (Figures 10-14).

While the corrosion rates of both SS 304L and Inc. 718 remain relative low over the course of exposure to the cooling water loop, those of Al6061 are undesirably high. Consider the 0.062" (approx. 1,600 μm) wall thickness Al6061 tube proposed as a conduit material for He/tritium in the APT project. Using a corrosion rate of 400 μm/year (Figure 13; 10/27/95, uniform corrosion, non-conservative) the wall thickness will decrease by

50% in 2 years. If corrosion is localized (which is the known breakdown mechanism for Al alloys) and the true rate is closer to $2.5x10^3$ µm/year, then a $1mm^2$ pit could easily breach the tube wall in less than a year. It should be noted that these results are preliminary and further testing is required to confirm these rates. Visual examination of the Al6061 corrosion probes when they are available will also be useful to help confirm the actual corrosion rate of this material in this environment.

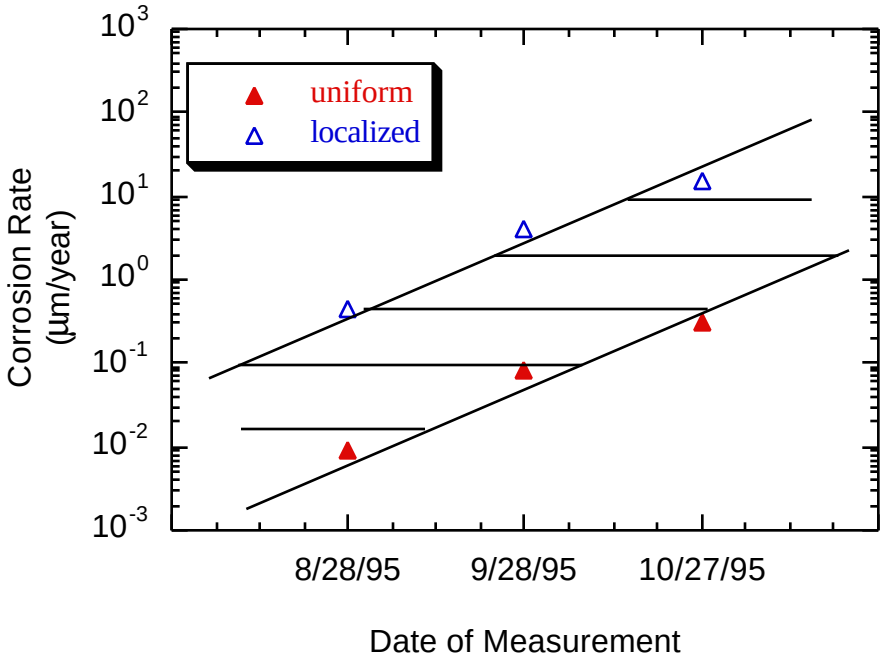

Figure 10 Corrosion rate vs. beam time for Stainless Steel 304L for both the uniform and localized analyses

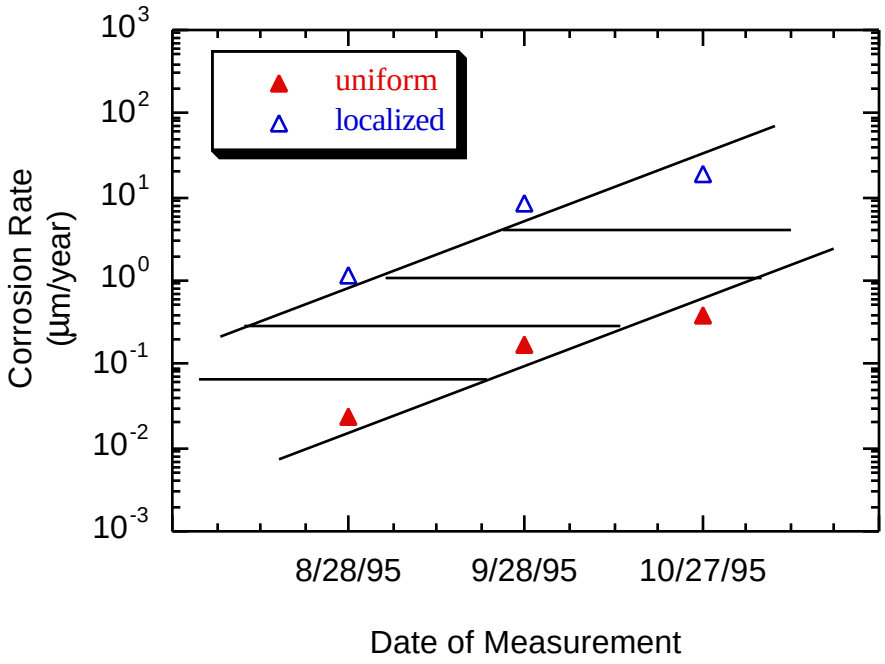

Figure 11 Corrosion rate vs. beam time for Inconel 718 for both the uniform and localized analyses

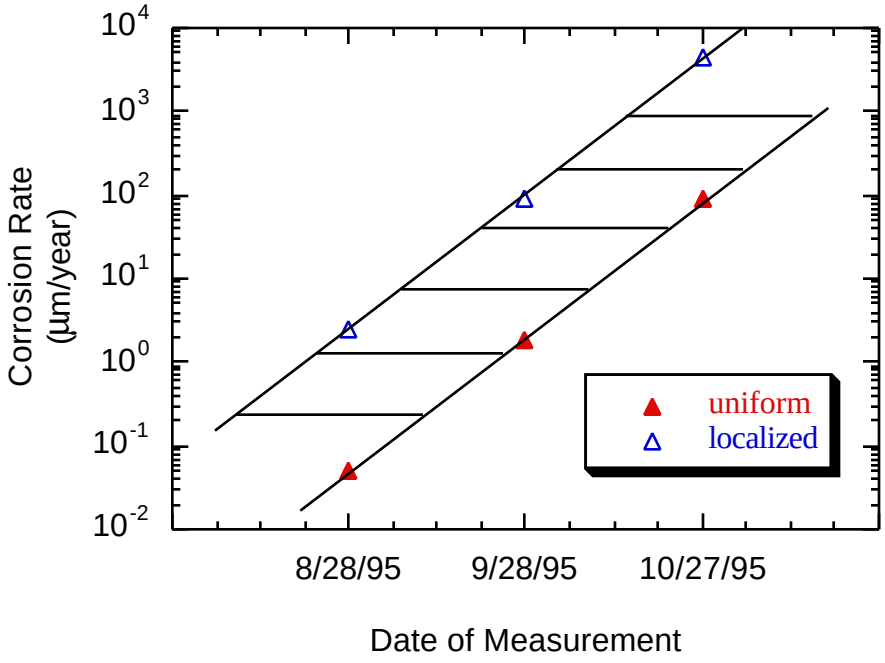

Figure 12 Corrosion rate vs. beam time for 99.95% Cu for both the uniform and localized analyses

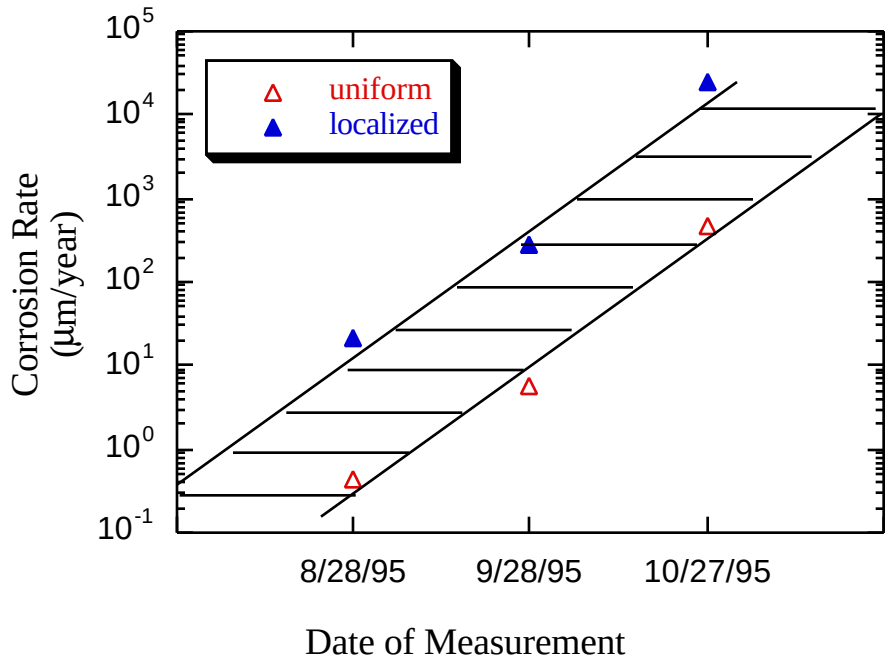

Figure 13 Corrosion rate vs. beam time for Aluminum 6061 for both the uniform and localized analyses

Corrosion Rates in Supply Stream vs. Return Stream The OCP as a function of time for the Cu corrosion probe in the supply stream is shown in Figure 14. At time = 0 in this plot, the degrader was out of the beam and the water was not being irradiated. At approximately the 2500 second mark the beam was turned off so that the degrader could be placed in the beam. Shortly thereafter, the beam was turned back on as shown in this plot. The OCP was continuously monitored through this procedure, however, no deviation in the OCP vs. time record is apparent after the degrader is placed in the beam. The OCP as a function of time for the Cu corrosion probe in the return stream bucket is shown in Figure 15. As before, at time = 0 in this plot, the degrader was out of the beam and the water was not being irradiated. At approximately the 200 second mark the degrader was lowered into position and the beam was turned on. In contrast to the supply stream data, a sharp increase in the OCP of the Cu sample is observed soon after the beam is turned on.

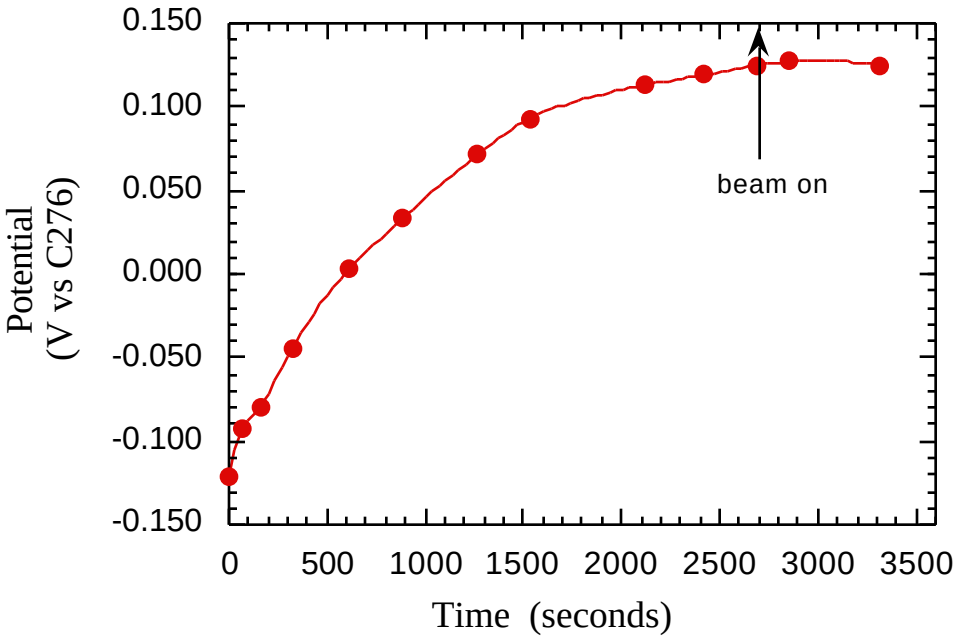

Figure 14 The open circuit potential vs. time data for Cu, supply stream bucket (measurement date: 8/22/95)

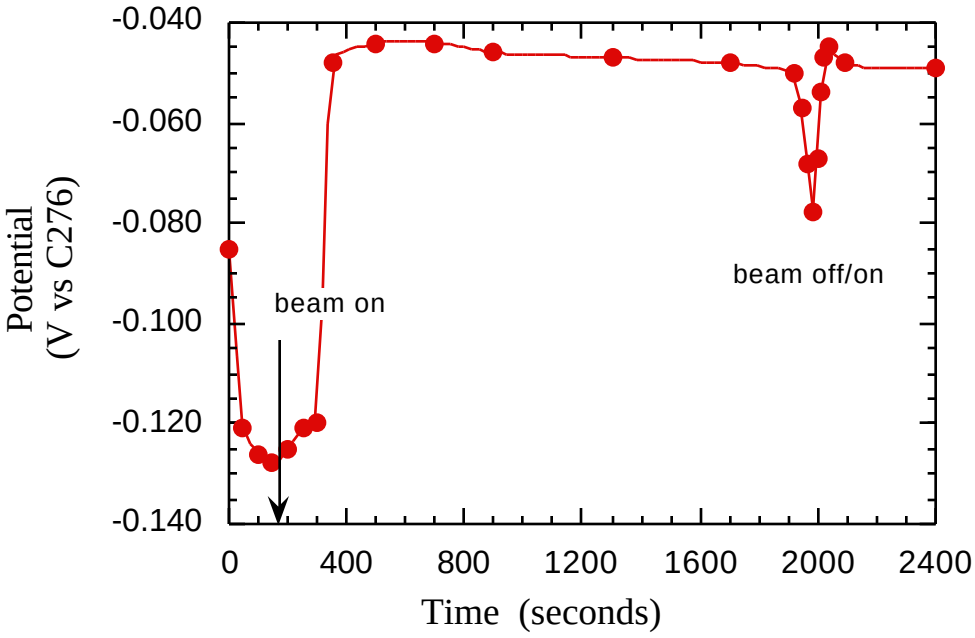

Figure 15 The open circuit potential vs. time data for Cu electrode in return stream bucket (measurement date: 8/22/95)

After approximately 300 seconds of irradiation a steady state value was achieved. Moreover, at approximately the 1900 second mark the beam was briefly turned off and the OCP began to decrease until the beam was turned back on at the 2000 second mark. Shortly thereafter the OCP returned to its steady state "beam on" value. This response is consistent with an increased concentration of oxidizing species such as, hydrogen peroxide, in the degrader cooling water**[5,11]**. Further, because no increase in the OCP was observed in the supply stream data after the beam was turned on, these oxidizing radiolysis products must either have a short half life or be consumed by the time they reach the supply stream corrosion probes. Therefore, because the return stream corrosion probes are exposed to higher concentrations of cathodic reactants, it is likely that the corrosion rates of materials on the return side of the beam will be higher than those on the supply side. It should also be noted that because the OCP of the C-276 reference electrode will also increase with an increased concentration of oxidizing species, that the absolute change in the OCP (Figure 15) may be greater.

After an additional 1 hour of irradiation to insure steady state, an EIS experiment was performed following each OCP vs. time record. The results from these experiments were analyzed in the same manner as those above for uniform corrosion (non-conservative). As presented in Figure 16, the corrosion rate of the Cu electrode in the return stream with the beam on was found to be 5 times greater than that of the Cu electrode in the supply stream with the beam on. Also presented in Figure 16 are the corrosion rates for these same samples taken on the previous day (8/21/95) with the beam off. This plot demonstrates the effect of oxidizing radiolysis products on the measured corrosion rates. As shown in Figure 16 the supply side corrosion rates are independent of degrader irradiation. This finding is further indication that the oxidizing radiolysis products must either have a short half life or be consumed by the time they reach the supply stream

corrosion probes. Unfortunately, problems with the flow rate in the degrader required daily flow reversals after 8/24/95. This procedure did not allow the long term comparison

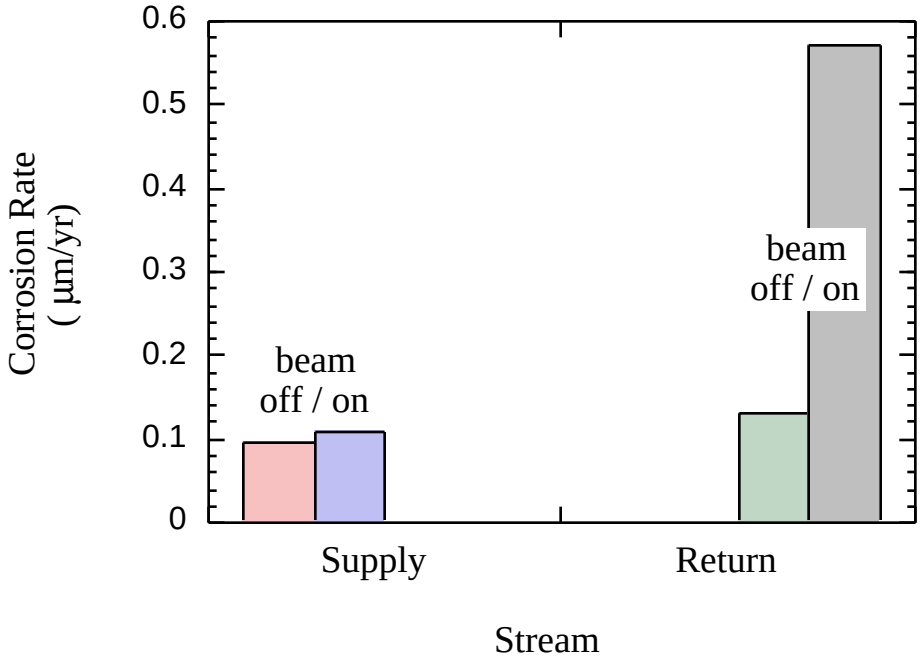

Figure 16 Comparison between supply and return stream corrosion rates for Cu electrodes. Plot shows both the beam off data (8/21/95) and beam on data (8/22/95) for the same electrode.

between the corrosion rates of materials in the supply stream vs. those in the return stream as originally planned.

Solution Conductivity Measurements Solution conductivity measurements were made with a specially constructed corrosion probe. While the probe housing was identical to that used in the corrosion measurements, three electrodes of equal size were made of Hastelloy C276 (16 at% Mo, 15.5% Cr, 5.5% Fe, 3.8% W, bal. Ni) and mounted onto the housing. This conductivity probe was calibrated in NaCl based solutions of various concentration (i.e. conductivity) and volume in order to determine its "cell constant".

To Calibrate the probe, the solution resistance between the electrodes was measured with EIS at a frequency above the high frequency break point. This data is presented in Table 3 for the NaCl solutions as a function of solution volume (Figure 17). From the EIS

Table 3 Solution compositions/conductivities used for calibration of conductivity probes.

solution #	Cl^- concentration milli-M	theoretical. conductivity $(ohm\ cm)^{-1}$
1	10	$1.26x10^{-3}$
2	1.0	$1.26x10^{-4}$
3	0.1	$1.26x10^{-5}$
4	0.01	$1.26x10^{-6}$

solution resistance measurements and the theoretical conductivity a cell constant was obtained using Ohm's Law:

$$R = \frac{\rho L}{A} \qquad \rho = \frac{1}{\sigma} \qquad \text{Eq. 3}$$

where: ρ = resistivity; σ = conductivity. By rearranging Equation 3 the cell constant was then obtained:

$$\left(\frac{L}{A}\right)_{vol,\ \sigma} = R_{sol} \cdot \sigma_{theo} \qquad \text{Eq. 4}$$

where: L/A is the cell constant (cm^{-1}), R_{sol} is the solution resistance (ohms), σ_{theo} is the theoretical solution conductivity in $(ohm\ cm)^{-1}$ calculated from the transference numbers**[18]**. The solution conductivity of the cooling water was then obtained from Equation 4 above, and the solution resistance between the conductivity probe electrodes from EIS (Figure 18). Because the cell constant varied with solution resistivity, Figure 17 was used to establish which conductivity curve most closely approximated the data. The cell constant for this at high volume (Figure 18) was then used to determine the solution conductivity of the cooling water loop. For example: an EIS conductivity probe

measurement of $4.0x10^{3}$ ohms most closely approximates the calibration measurement made for a solution resistance of $1.26x10^{-5}$ (at high volume) and, therefore a cell constant of 0.055 (from Figure 18) would be used to obtain the solution conductivity.

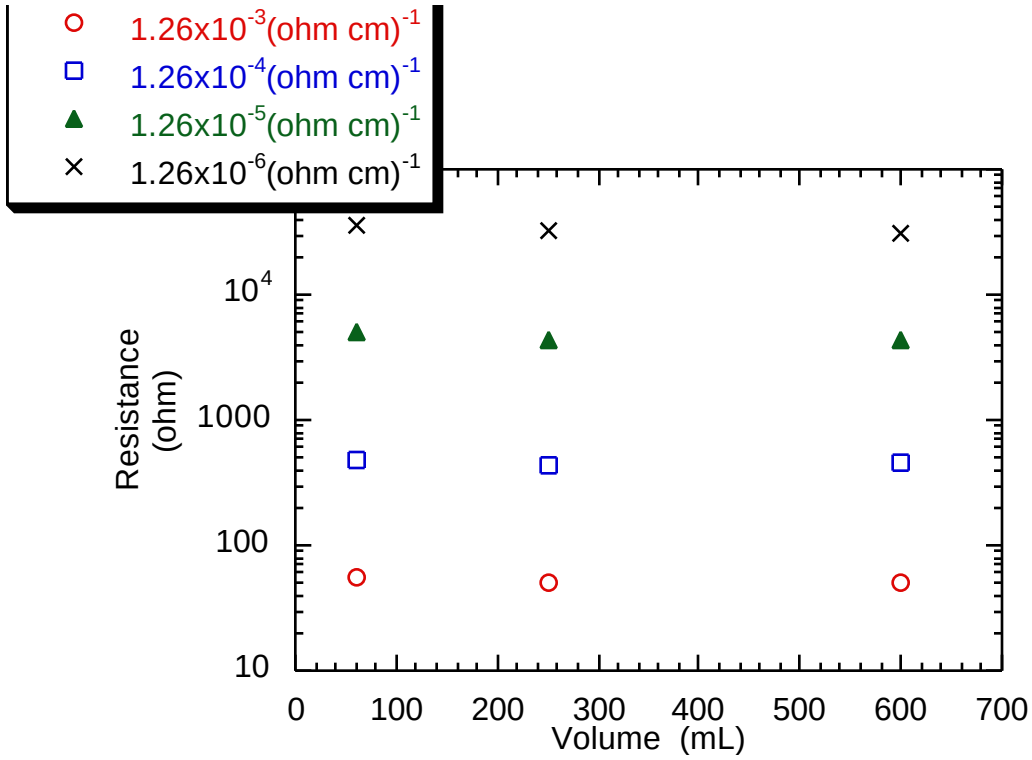

Figure 17 Measured solution resistance between the electrodes in the conductivity probe for NaCl based solutions of various conductivity as a function of solution volume.

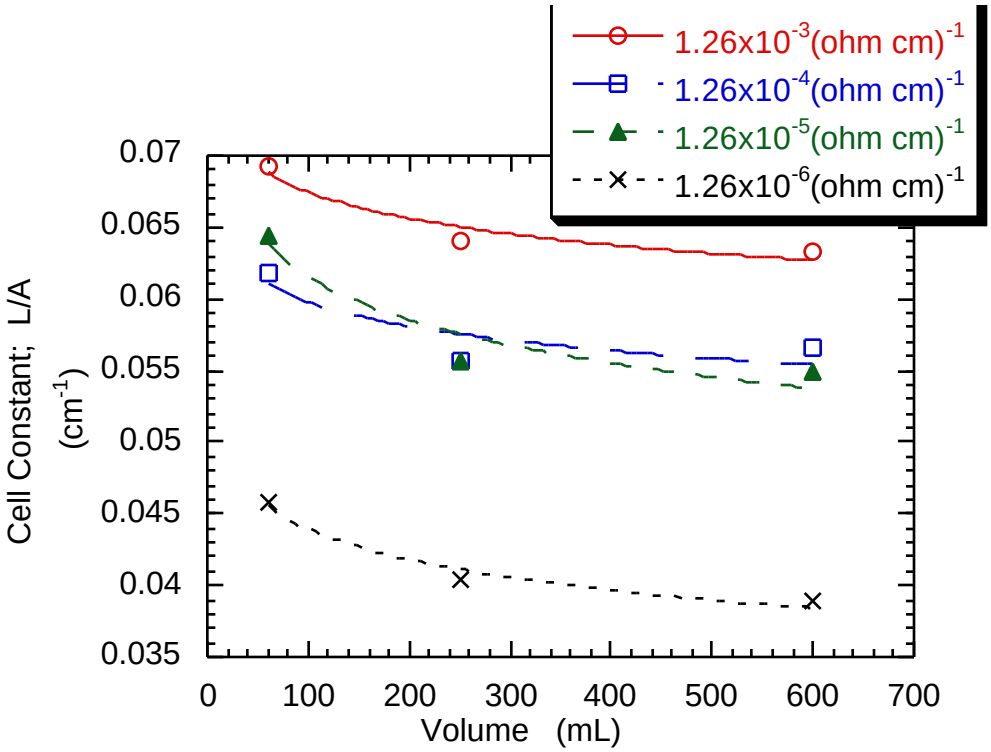

Figure 18 Conductivity probe cell constant as a function of solution volume and conductivity.

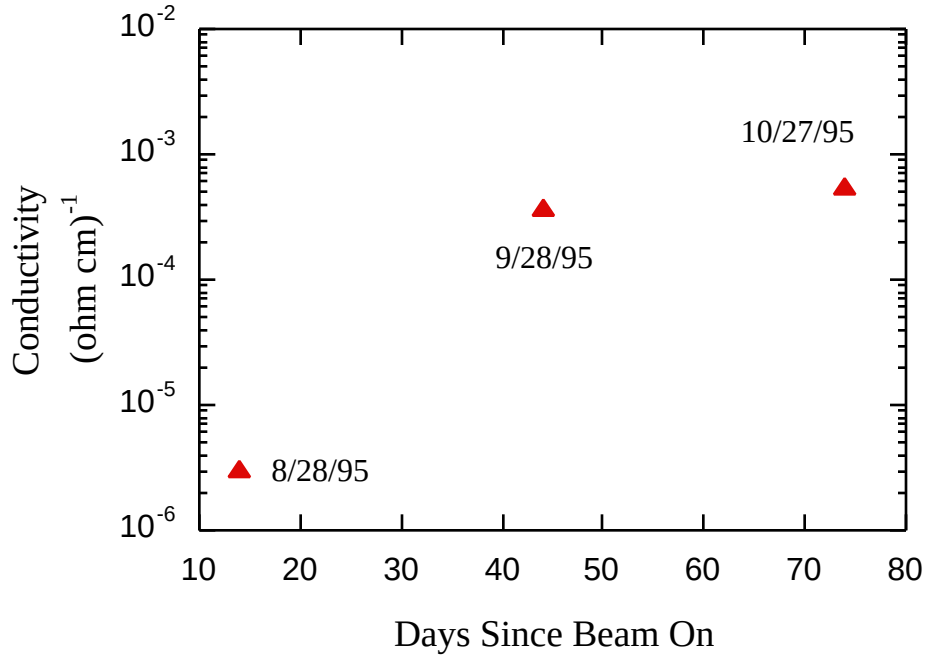

Figure 19 Measured solution conductivity as a function of beam time.

The solution conductivity results for the return stream as a function of immersion time are presented in Figure 19. Initially, the solution conductivity was approximately $3x10^{-6}$ (ohm cm)$^{-1}$. This value decreased markedly over the test period to a final conductivity of $6x10^{-4}$ (ohm cm)$^{-1}$. The trend may owe to a build up of radiolysis products, metal ions, or both and correlates well with the corrosion rate and OCP measurements. Future experiments will include an analysis of ion concentrations in solution (via ion coupled plasma) and solution pH measurements as a function of time will help to establish the basis for the observed change in solution conductivity.

Summary

This work was a proof of concept for our APT prototypical corrosion rate measurements to begin in the Summer of 1996. We have: **1)** developed a corrosion probe / electrodes that will operate reliably in a radioactive cooling water loop, **2)** developed a "floating" - portable corrosion measurement system that employs EIS a non-destructive technique for measuring corrosion rates and, **3)** developed a data analysis model so that corrosion rate and solution resistivity can be measured in the APT prototypical environment. This corrosion measurement system was demonstrated by measuring the corrosion rates of various engineering materials in the cooling water loop for a water degrader in the A6 target station at LANSCE.

A comparison between the corrosion rates of Cu electrodes in the supply stream versus the return stream in the cooling water loop for a degrader in the A6 target station at LANSCE have demonstrated the role of radiolysis products in the corrosion process. In addition, the long term effects of water irradiation were found to increase cooling water conductivity by several orders of magnitude over the test period. It is uncertain if this increase in conductivity owes to an increasing concentration of long lived radiolysis

products (such as hydrogen peroxide), a change in solution pH, the build up of corrosion products in the cooling water loop or some combination of all three.

Results have also shown that the corrosion rate of aluminum 6061 increased by 3 orders of magnitude during the 4 months of immersion in the degrader cooling water. The corrosion resistance of this alloy at the end of the test period was classified as **Fair** to **Unacceptable** depending on the data analysis used (localized corrosion vs. uniform corrosion). In comparison, 304L SS and Inc. 718 maintain **Outstanding** to **Excellent** classifications during the test period even assuming a conservative non-uniform corrosion (pitting) on the sample surface. To verify these results a visual inspection of the corrosion electrodes will be necessary. This will be carried out once the bucket radiation levels have dropped to a low enough level for human exposure.

Future Work

- "Post Mortem" Analysis of Corrosion Electrodes to Determine Whether or not Pitting Corrosion Exists
- Development of "In Beam" Corrosion Probes to Allow Measurement of Corrosion Rates While Exposed to the Proton Beam
- Development of pH Probe to Measure Changes in Cooling Water pH during the Test Period
- Examine the Effect of Hydrogen Water Chemistry on Corrosion Mitigation in a Prototypical Spallation Target Cooling Water Loop
- Measurement of Corrosion Rates on Proposed APT Materials (W, HT-9, 316NG, Al6061, Inconel 718, 304L SS) in a Prototypical Spallation Target Cooling Water Loop
- Laboratory Corrosion Rate Measurements in Simulated Spallation Target Cooling Water

- Measure the Corrosion Rates of Potential Galvanic Couples in Simulated Spallation Target Cooling Water

References

1 J.L. Magee, A. Chatterjee, in Kinetics of Nonhomogeneous Processes, G.R. Freeman ed., John Wiley & Sons, New York, pp171-214, 1987.

2 H. Christensen, **Nuclear Technology**, vol. 109, pp. 373-82, 1994.

3 T.K. Yeh, D.D. Macdonald, A.T. Motta, **Nuclear Science and Enginering**, vol. 121, pp 468-82, 1995.

4 W.G. Burns, P.B. Moore, **Radiation Effects**, vol. 30, pp. 233-42, 1976.

5 R.S. Glass, G.E. Overturf, A. Van Konynenburrg, R.D. Mccright, **Corrosion Science**, vol. 26, no. 8., pp. 577-90, 1986.

6 H. Christensen, **Radiation Physical Chemistry**, vol 18, no. 1-2, pp.147-58, 1981.

7 W.G. Burns, W.R. Marsh, W.S. Walters, **Radiation Physical Chemistry**, vol. 21, no. 3, pp. 259-79, 1983.

8 M. Fox, "Water Chemistry and Corrosion in BWR's", *Corrosion/83*, paper no. 121, NACE, Houston, 1983.

9 M.E. Indig, J.E. Weber, **Corrosion**, vol. 41, no. 1, pp. 19-30, 1985.

10 J.J. Taylor, **EPRI Journal**, vol. 11, no. 3, pp. 54-55, 1986.

11 D.D. Macdonald, **Corrosion**, vol. 48, no. 3, pp.194-205, 1992.

12 D.D. Macdonald, H. Song, K. Makela, K. Yoshida, **Corrosion**, vol. 49, no. 1, pp. 8-16, 1993.

13 J.R. Macdonald, Impedance Spectroscopy, Wiley Publishing, New York, 1987.

14 I. Epelboin, C. Gabrielli, M. Keddam, H. Takenouti, "Alternating-Current Impedance Measurements and Corrosion Rate Determination", in Electrochemical Corrosion Testing, ASTM STP 727, F. Mansfeld & U. Bertocci eds., ASTM, Ohio, pg. 150-66, 1981

15 D.D. MacDonald, M.C.H. Mckubre, "Electrochemical Impedance Techniques in COrrosion Science" in Electrochemical Corrosion Testing, ASTM STP 727, F. Mansfeld & U. Bertocci eds., ASTM, Ohio, pg. 110-59, 1981

16 D.D. MacDonald, "Theoretical Analysis of Electrochemical Impedance", *Corrosion87*, paper #479, NACE, Houston, 1987.

17 M.G. Fontana, Corrosion Engineering, McGraw-Hill, New York, pp. 171, 1967.

18 J. Newman, Electrochemical Systems, Prentice Hall International Series, Englewood Cliffs, NJ, 1973.